ISBN: 978-3-95450-243-1 ISSN: 2226-0374 doi:10.18429/JACoW-COOL2021-S503

AD/ELENA ELECTRON COOLING EXPERIENCE DURING AND AFTER CERN LONG SHUTDOWN (LS2)

D. Gamba*, L. Bojtar, C. Carli, B. Dupuy, A. Frassier, L. V. Joergensen, L. Ponce, G. Tranquille,
CERN, 1211 Geneva, Switzerland

Abstract

Electron cooling is a key ingredient of the Antimatter Factory at CERN, now composed of the AD and ELENA rings, both featuring an electron cooler. After the successful commissioning of the ELENA ring and electron cooling with antiprotons in 2018, the facility was shutdown for the CERN long shutdown (LS2). In the meantime, ELENA has been operating with H^- ions generated from a local source and electron cooling of these H^- was demonstrated. The facility has restarted with antiproton operation during summer 2021, and it is now delivering 100 keV production beams through newly installed electro-static extraction lines to all the experiments for the very first time. We will give an overview of the experience gained and difficulties encountered during the restart of the AD and ELENA electron coolers. The experience with electron cooling of H^- beam in ELENA and the comparison with antiproton cooling will also be presented.

INTRODUCTION

The Antimatter Factory at CERN is a unique facility that provides antiproton beams to several experiments [1]. The facility, originally composed only by the Antiproton Decelerator (AD) [2], was complemented with the Extremely Low ENergy Antiproton (ELENA) ring [3] which was successfully commissioned in 2018 [4]. The AD provides about 3×10^7 antiprotons in a single bunch at 5.3 MeV kinetic energy approximately every two minutes. The ELENA ring allows to further decelerate the antiprotons down to 100 keV kinetic energy and produces 4 bunches of about 5×10^6 antiprotons per bunch, which are distributed to up to 4 experiments at the same time. The cycle length of ELENA, of about 15 seconds, falls in the shadow of the next AD cycle.

Stochastic cooling (in AD) and electron cooling (both in AD and ELENA) are used on several plateaus placed at injection (in AD), during the deceleration process, and before extraction in order to counteract the adiabatic emittance increase as well as possible heating effects.

Till the end of 2018, GBAR [5] was the only experiment connected to ELENA. During CERN Long Shutdown 2 (LS2), all AD experiments were connected to ELENA with the installation of electrostatic transfer lines. Despite the unavailability of antiprotons during LS2, the ELENA ring could still be operated with beams from of a local H^-/p source [6,7]. This allowed for progressing in the optimisation of beam performance in the ELENA ring, including e-cooling, as well as to commission the transfer line beam transport well before the arrival of the first antiproton beam after LS2.

The first proton beam for pbar production after LS2 was delivered at the end of June 2021. In the following weeks the AD operation was restored, including the setup of AD stochastic cooling [8] and electron cooling. The first pbar beam was delivered to ELENA mid August 2021 and 100 keV antiproton beams were available for users starting on August 23rd, as scheduled. During this short time, only minor adjustments of the previously prepared H^- cycle were necessary to decelerate and cool pbars, demonstrating that H^- beams can be used for optics and cooling studies in ELENA without the need of pbars.

In the following sections, the achieved beam performance of the facility will be outlined followed by observations of e-cooling related aspects during the restart in 2021.

BEAM PERFORMANCE IN 2021

During the run, further optimisation of both AD and ELENA cycles allowed to improve the overall performance of the facility. By construction, the characteristics of the beam delivered to experiments are defined by the e-cooling performance and heating effects (like Intra-Beam Scattering (IBS)) on the extraction plateau of ELENA, while the final intensity is driven by the efficiency of antiproton production and collection (in AD), and deceleration. For this, stochastic and electron cooling play a key role to at least counteract the adiabatic increase of the beam transverse and longitudinal emittances. The final AD and ELENA cycle deceleration efficiency are presented in Fig. 1 and Fig. 2, respectively. In AD the beam intensity is measured by a Cryogenic Current Comparator (CCC) [9], which allows to measure the beam current also while the beam is unbunched, while in ELENA the beam intensity is estimated by the Low Level Radio Frequency (LLRF) system which only works when the beam is bunched and does not take into account for longitudinal

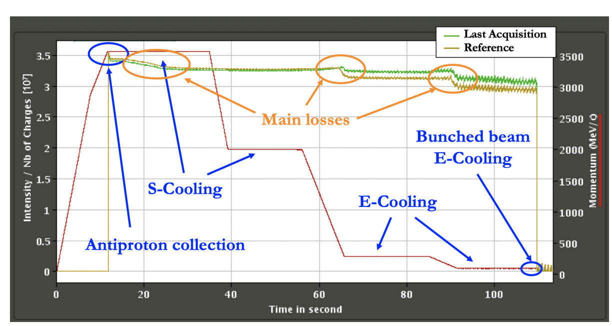

Figure 1: Beam intensity (in units of 10^7 charges) along a typical AD cycle. The main observations are highlighted.

* davide.gamba@cern.ch

ISBN: 978-3-95450-243-1 ISSN: 2226-0374 doi:10.18429/JACoW-COOL2021-S503

distribution variations and therefore has a lower accuracy than the AD CCC.

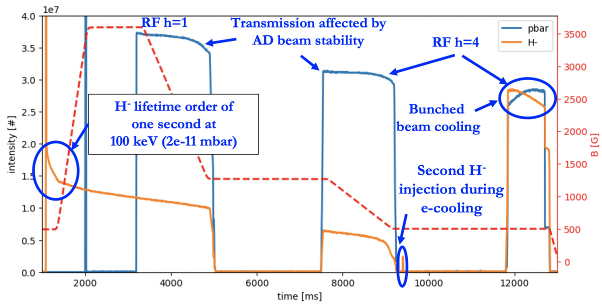

Figure 2: H^- (orange) and pbar (blue) beam intensity along a typical ELENA cycle (dashed red). The main observations are highlighted.

During the 2021 run it was not possible to re-establish the same pbar production and/or AD injection efficiency that was achieved in 2018, which was as high as 5e7 pbars injected, while the final AD deceleration efficiency of about 85% is close or better than what was achieved in the past. In AD, the main losses appear on the injection plateau, likely due to the limited longitudinal acceptance of the stochastic cooling system, and during the 2 GeV/c to 300 MeV/c, and 300 MeV/c to 100 MeV/c ramps, likely due to poor cooling performance on the tails of the beam distribution. In ELENA, the achieved transmission was of the order of 80%, which is much higher than the 60% from the design [3] and the 50% achieved in 2018 [4].

The typical distribution of single bunch intensities over 7 days of operation is shown in Fig. 3. In this case, the bunch intensity is measured by two beam current transformers [3] installed on the two extraction lines, named LNE50 and LNE00. GBAR is presently the only experiment in the LNE50 line. The discrepancy in the average beam intensity between GBAR and the other experiments is due to the presence of a partially-intercepting beam profile monitor upstream the intensity monitor but also due to systematic calibration and measurement issues on the two LNE50 and LNE00 pickups, which are being investigated.

Other main beam characteristics at ELENA extraction are summarised in Table 1 together with design values.

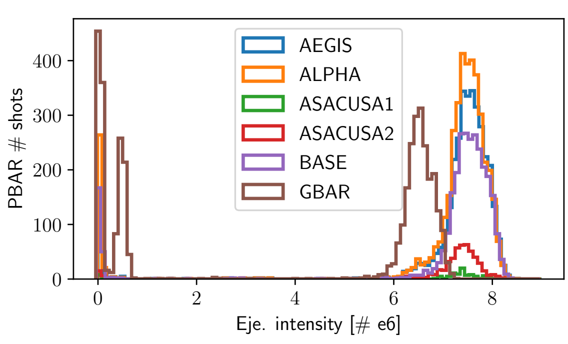

Figure 3: Typical distribution of ELENA extracted bunch intensities per experiment over one week of operation.

Table 1: Design [3] and estimated beam parameters at ELENA extraction at the end of 2021 run for the pbar cycle.

Parameter	Design	Obtained
Q_x/Q_y	$\approx 2.3/\approx 1.3^a$	2.38/1.39
Cycle duration [s]	20	<15
Injected intensity [pbars]	3e7	≈3e7
Efficiency [%]	60	≈80
Extracted bunches [#]	4	4
Bunch population [pbars]	4.5e6	≈7e6
$\Delta p/p_0$	5e-4	≈4.5e-4
Bunch length (rms) [ns]	75	<75
ϵ_{phys} x/y [μm]	1.2/0.75	≈2/≈2

[a] With sufficient tuning range to choose working point in vicinity.

E-COOLERS AND INSTRUMENTATION

The main parameters of the AD and ELENA e-coolers are summarised in Table 2.

The AD e-cooler is the oldest built at CERN: it was used in the Initial Cooling Experiment (ICE) in 1977-80, then used in LEAR (1982-97) and finally moved to the AD where is being used since 1999. Due to the critical spare parts situation, a new e-cooler for AD is being designed [10]. During LS2, it was planned to already replace the present electron collector with one compatible with the new e-cooler design. Unfortunately, the pandemic situation, and high-voltage issues discovered during testing of the first prototype did not allow to perform this exchange. This would have been the occasion to also replace the thermionic cathode in the electron gun, which is now being operated for several years. However, the unavailability of the new collector and the overall good performance of the present cathode did not justify to break the vacuum, which is always considered to be a risky operation for the long baking time needed to recover good vacuum (typically of the order of 10^{-11} mbar).

The ELENA e-cooler [11–13] was commissioned in 2018 [14], and did not require any special modification. Therefore, no modifications nor major maintenance was done in either AD and ELENA e-cooler during LS2.

The key instrument for the setup and optimisation of cooling is the longitudinal Schottky system. In AD this is realised by looking at the second (300 MeV/c) or eighth (100 MeV/c)

Table 2: AD and ELENA E-Cooler Main Parameters

Parameter	AD		ELENA	
Ion p [MeV/c]	300	100	35	13.7
Ion E_k [MeV]	46.8	5.3	0.635	0.1
e^- E_k [keV]	25.5	2.9	0.355	0.055
β_{rel}	0.305	0.106	0.037	0.015
I_{e^-} [mA]	2.5e3	100	5	1
Cooler L [m]	1.5		1	
Ring L [m]	182.43		30.41	
Gun B [G]	590		up to 1000	
Drift B [G]	590		100	
e^- beam r [mm]	25		8 to 25	

ISBN: 978-3-95450-243-1 ISSN: 2226-0374 doi:10.18429/JACoW-COOL2021-S503

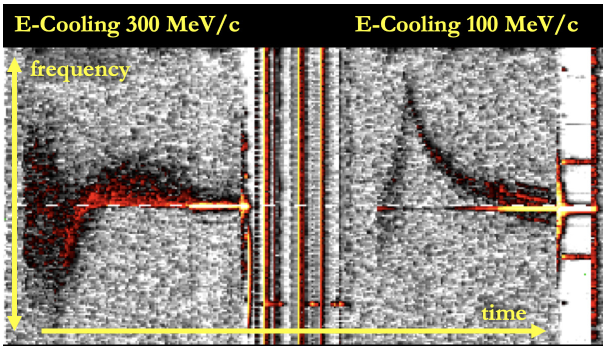

Figure 4: Example of AD longitudinal Schottky measurement along the two e-cooling plateaus.

revolution harmonic on the signal generated by the ring longitudinal pickup [15]. The signal is downmixed to 50 kHz central frequency at each cooling plateau, allowing for observing the Schottky all along the cycle and in real time on a simple spectrum analyser and by simple digital signal processing as shown in the example waterfall acquisition in Fig. 4. The ELENA longitudinal pickup [16] turned out to have a lower Signal-to-Noise Ratio (SNR) than expected. Instead, the Schottky signal could be easily seen by using a single ELENA Beam Position Monitor (BPM) [17] sum signal or by merging the signal of several pickup which allowed to further gain in SNR [18].

The transverse beam profiles are measured by scrapers [19, 20], which are devices that measure the secondary emission of a moving blade progressively entering the beam pipe. Due to the destructive nature of those devices, and the very low repetition rate of the machine, those devices cannot be easily used for measuring the time-evolution of the cooling process. On the other hand, they allow for estimating the transverse cooling performance and therefore guide the cooling optimisation by comparing the transverse profile measured before cooling with profiles measured at subsequent shots with cooling, as shown in the following section.

Semi-intercepting micro-wire monitors (also called SEM) [21] are also installed in the AD-to-ELENA and ELENA-extraction transfer lines. Only about 10% of the beam intensity is lost per crossing. This allowed to develop a multi-profile Twiss measurement to characterise the extracted beam, as shown for example in Fig. 5. Profile monitors in the AD-to-ELENA transfer also allowed for AD e-cooling optimisation at 100 MeV/c without the need of scraper measurements. They also allowed for tracing back poor shot-to-shot ELENA injection efficiency to a poor current regulation of the AD extraction septa.

The e^- beam position in the e-cooler drift section could be measured by the thereby installed BPMs after imprinting an e^- intensity modulation. The modulation was generated by installing a coupling transformer on the cable supplying the e^- gun grid electrode voltage, as shown in Fig. 6. The frequency of the modulation was generated by the BPM acquisition system locked to the beam revolution frequency and for a user-selectable harmonic. This allowed to measure the e^- orbit on the very same pbar BPM acquisition system without the need of dedicated system. Following first promising experiments in ELENA in 2019, this technique was deployed on all CERN e-coolers during LS2, and this allowed to quickly establish cooling by carefully matching the ion and e^- orbits.

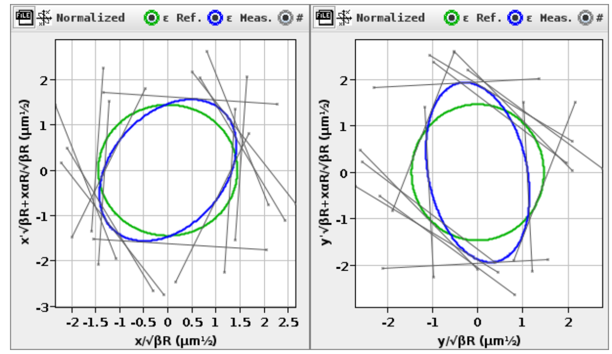

Figure 5: Horizontal (left) and Vertical (right) transverse Twiss measurement (blue) and nominal (green) presented in normalised phase space. Gray lines correspond to beam sizes measured by several SEM along the LNE00 transfer line.

E-COOLING OBSERVATIONS

E-cooling setup and adjustment in AD was reported in the past as a lengthy process, especially at 300 MeV/c where the nearby orbit corrector strength is limited [22]. Thanks to the e^- orbit measurement deployed during LS2, it was possible to start from reducing the orbit corrector strength, and then add the minimum strength necessary to match the e^- and pbar orbits within a few mm. With subsequent adjustments of the e^- energy by looking at the longitudinal Schottky spectra evolution, it was then rather fast to establish first longitudinal cooling. Transverse cooling was then optimised mainly by scanning the pbar angle in the e-cooler in steps of the order of 0.1 mrad and by continuously looking at scraper data or, only at 100 MeV/c, by looking at the transverse beam profile measured by a SEM in the AD-to-ELENA transfer line.

A typical Schottky waterfall after optimisation of the 300 MeV/c cooling is shown in Fig. 7. The total length of the cooling plateau is about 15 s, as also shown in Fig. 1. The initially wide frequency spread observed in the Schot-

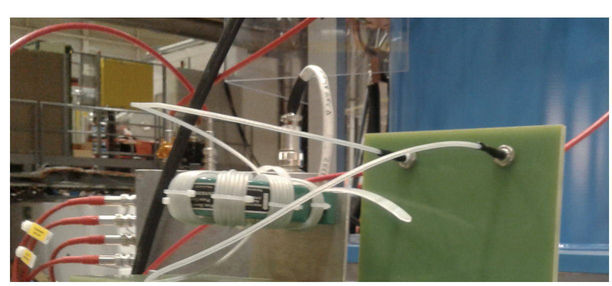

Figure 6: Coupling transformer installed on the high voltage cable powering the grid electrode at the ELENA e-cooler.

ISBN: 978-3-95450-243-1 ISSN: 2226-0374 doi:10.18429/JACoW-COOL2021-S503

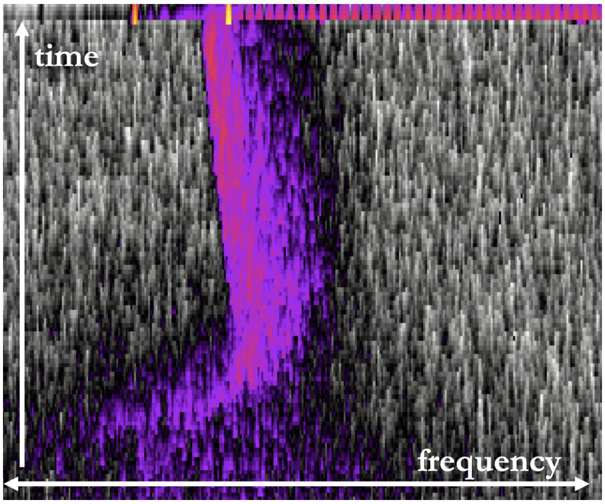

Figure 7: Schottky spectra ($h = 2$) evolution along the 15 s-long 300 MeV/c plateau.

tky is quickly reduced to about 10^{-4} rms, but then a tail on the high-frequency side of the spectrum develops and this is later cooled back. A sharp edge instead develops on the low-frequency side of the spectra, and remains as such but for a small drift in frequency along the plateau. Such a behaviour could be explained by the interplay of e^- space charge, and pbar longitudinal and transverse cooling, as shown in preliminary simulations presented in [23].

Transverse cooling at 300 MeV/c was confirmed by looking at the transverse beam profile measured with scraper without and with cooling on, see Fig. 8. Note that an ideal scraper measurement of a monochromatic Gaussian beam would look like a perfect half-Gaussian. Deformation with respect to this ideal situation can be due to non-Gaussian beam profile, or non-zero dispersion at the location of the scraper [24]. The not-cooled profiles measured in Fig. 8 seems to suggest a rather hollow beam distribution before cooling. On the other hand, inconsistencies have been seen in the data provided by the scraper control system, therefore

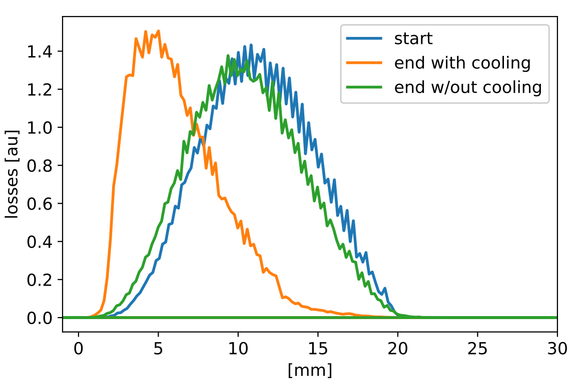

Figure 8: Pbar horizontal half-profile measured by the AD scraper at 300 MeV/c at the beginning (blue) and end (orange and green) with (orange) and without (green) cooling with coasting beam. The Twiss β function at the scraper is about 5 m and zero dispersion.

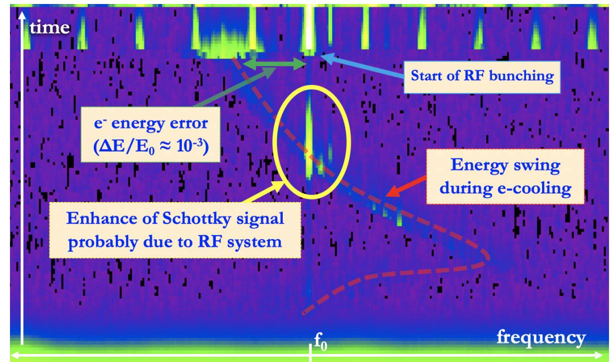

Figure 9: Schottky spectra ($h = 8$) evolution along the 15 s-long 100 MeV/c plateau.

investigation on the accuracy of such a measurement and possibly crosscheck with other methods should be envisaged before drawing any quantitative conclusion.

Due to a tight commissioning schedule, it was found that bunched-beam cooling on the whole 100 MeV/c plateau was the faster way to deliver good beams to ELENA, and so allowing to start its commissioning. The nominal un-bunched beam cooling was then re-established during the physics run. Even then, bunched-beam cooling was kept for about 2.5 s before extraction in order to obtain low bunch length at extraction. Figure 9 shows the Schottky waterfall evolution on the 100 MeV/c plateau in this final configuration. Note that the central beam energy as seen by the Schottky spectra drifts toward about 10^{-3} higher relative frequency before being dragged back to lower frequencies. This beam energy swing was already observed in the past and no clear explanation is known, but it might still be due to the interplay between e^- space charge and cooling process. Simulation studies should be envisaged to clarify this observation. When the beam crosses the programmed RF frequency, the Schottky spectra in Fig. 9 looks enhanced. This is a new effect observed after LS2, and it is believed to be due to the not-full closure of the gap relay in the newly installed Finemet cavity [25] used for the beam deceleration. No sizeable perturbation of the cooling process were associated to this perturbation. Instead, a more serious perturbation on the cooling at 100 MeV/c was the shot-to-shot drift of the final beam energy after cooling, which could sensibly deviate from the central RF frequency, as also visible in Fig. 9, and which therefore had detrimental effect on the re-bunching, on the subsequent bunch-beam cooling, and finally on the overall beam transmission to ELENA. This perturbation was traced back to a sudden raise of the vacuum level in the e-cooler region from the nominal 10^{-11} mbar to up to about 10^{-9} mbar. Those variations were linked to vacuum activity in the stochastic cooling pickup and bunch-rotation cavities which are located in the nearby vacuum sectors. The beam energy could be re-adjusted by correcting the e^- acceleration voltage while nominal vacuum level was re-established. Fortunately, such an event were rare (once every few days on average) and of short duration (up to one hour), therefore the impact on the physics was limited.

ISBN: 978-3-95450-243-1 ISSN: 2226-0374 doi:10.18429/JACoW-COOL2021-S503

The ELENA e-cooler was commissioned before the start of the pbar run using H^-. Despite previous observation of poor lifetime in LEAR [26,27], no clear sign of beam lifetime degradation due to interaction of H^- with the electron cooler e^- beam was observed. This observation is compatible with the expected low cross section for H^- electron detachment for electron energies below a few eV [28] to be compared with typical e-cooler e^- temperature of less than 0.1 eV.

Due to the slightly different mass of pbar and H^-, the programmed momentum on the cooling plateaus for the H^- cycle was increased by about 0.1% such as to obtain the same speed of H^- and pbar beams on the plateaus, and therefore keep the same settings for the electron energy for both cycle types. Apart from this correction, no noticeable difference in cooling performance were seen between H^- and pbar, except for lower equilibrium emittances for low intensity H^- beams.

Figure 10 shows the Schottky spectra evolution as a function of time on the ELENA intermediate plateau at 35 MeV/c both with and without cooling on. In this case, the initial revolution frequency is mismatched with respect to e^- energy, therefore, with cooling, the beam is dragged in about 800 ms to the e^--defined energy. From this dragging one can estimate a rather constant dragging force of about 6 meV/m, which is compatible with expected force as simulated in RF-Track [29] assuming the cooling parameters from Table 2.

Figure 11 shows several vertical scraper measurement along the 35 MeV/c plateau. The V-shape structure that appear in the middle of the overall profile seen in Fig. 11 could be an indication of non-zero vertical dispersion at the scraper location, or rather an accuracy issue of the scraper which should be further investigated. Similar behaviour as in Figs.10 and 11 was seen also in the horizontal plane and at the lowest momentum plateau of 13.7 MeV/c. In both the longitudinal and transverse phase space one can notice that equilibrium is reached rather quickly, after about 1 s, suggesting that ELENA cycle lengths could potentially be shorter.

Figure 12 shows the extracted transverse emittances as a function of bunch intensity observed along a typical day of operation and estimated from the beam size measured at the first SEM in LNE50 line and assuming the design Twiss β_x/β_y = 7.7/1.3 m at that location. A clear dependence between intensity and emittance is visible. This could be a first indication of the space-charge driven limitations discussed in the ELENA design [3] and which should be further investigated in the next run.

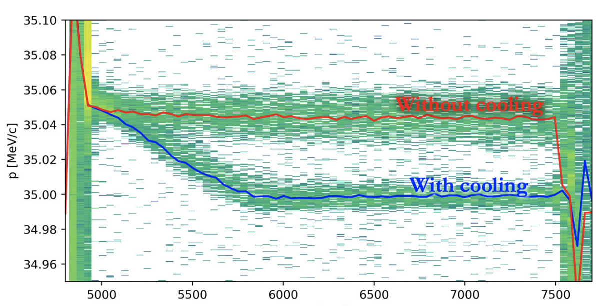

Figure 10: Comparison of Schottky spectra (h = 7) evolution at 35 MeV/c without (red) and with (blue) e-cooling on.

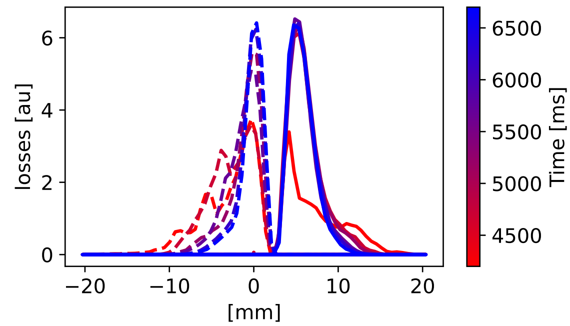

Figure 11: Vertical half-profile evolution (colour code) measured with scraper on the ELENA 35 MeV/c plateau with cooling. The scraper blade was intercepting the beam starting from negative (dashed) or positive (solid) position.

CONCLUSIONS

The AD and ELENA was successfully re-commissioned after LS2, and e-cooler performance comparable to pre-LS2 times were re-established. Schottky diagnostics was the preferred tool for e-cooling setup, despite of observations that are yet to be fully understood. Scraper measurements were found to be ambiguous at times. For the next run it is envisaged to re-establish the Ionisation Profile Monitor already installed in AD as an alternative and hopefully more effective way to measure the transverse emittance evolution along the cycle. The possibility of using H^- for the setup and optimisation of e-cooling in ELENA allowed to minimise the time needed to re-commission ELENA with pbars. During the next run it is envisaged to study and possibly reduce the beam emittance at extraction in order to match the design values.

ACKNOWLEDGEMENTS

The success of the AD and ELENA commissioning were made possible only thanks to many groups and people who worked with dedication and perseverance despite the pandemic situation and the planned commissioning over the summer-holiday period.

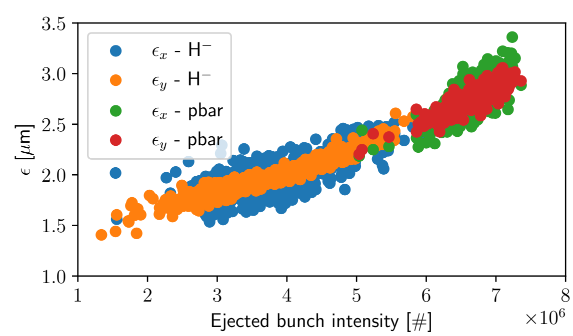

Figure 12: Transverse rms emittance estimate as a function of bunch intensity for H^- and pbar extracted from ELENA.

ISBN: 978-3-95450-243-1 ISSN: 2226-0374 doi:10.18429/JACoW-COOL2021-S503

REFERENCES

[1] M. Hori and J. Walz, "Physics at CERN's Antiproton Decelerator", *Prog. Part. Nucl. Phys.*, vol. 72, pp. 206 - 253, Sep. 2013.

[2] B. Autin *et al.*, "The Antiproton Decelerator (AD), a Simplified Antiproton Source (Feasibility Study)", CERN, Geneva, Switzerland, Rep. CERN-PS-95-36-AR, Nov. 1995.

[3] V. Chohan (ed.) *et al.*, "Extra Low ENergy Antiproton (ELENA) ring and its Transfer Lines: Design Report", CERN, Geneva, Switzerland, Rep. CERN-2014-002, Jan. 2014.

[4] D. Gamba *et al.*, "ELENA Commissioning", in *Proc. NA-PAC'19*, Lansing, MI, USA, Oct 2019, paper WEYBB1, pp. 626–631.

[5] P. Perez and Y. Sacquin, "The GBAR experiment: gravitational behaviour of antihydrogen at rest", *Classical and Quantum Gravity*, vol. 29, pp. 184008, Aug. 2012.

[6] A. Megía-Macías, R. Gebel and B. Lefort, "The ion source for the commissioning of ELENA ring", in *Proc. ICIS'2017*, Geneva , Switzerland, Oct. 2017, vol. 2011, no.1, p. 090014.

[7] D. Gamba *et al.*, "Operational experience with the ELENA ion source", in *AIP Conf. Proc. NIBS 2020*, Online, Sep. 2020, vol. 2373, no.1, p. 040005.

[8] W. Höfle *et al.*, "Recommissioning of the CERN AD Stochastic Cooling System in 2021 after Long Shutdown 2", *these proceedings*, Novosibirsk, Russia, Oct. 2021, Paper S302.

[9] M. Fernandes *et al.*, "Operation of a Cryogenic Current Comparator with Nanoampere Resolution for Continuous Beam Intensity Measurements in the Antiproton Decelerator at CERN", in *Proc. IPAC'18*, Vancouver, Canada, May 2018, paper THPML044.

[10] G. Tranquille *et al.*, "A New Electron Cooler for the CERN Antiproton Decelerator (AD)", *these proceedings*, Novosibirsk, Russia, Oct. 2021, Paper P2004.

[11] G. Tranquille *et al.*, "The ELENA Electron Cooler", in *Proc. IPAC'16*, Busan, Korea, May 2016, paper TUPMR006.

[12] G. Tranquille *et al.*, "Design and Optimisation of the ELENA Electron Cooler Gun and Collector," in *Proc. IPAC'16*, Busan, Korea, May 2016, paper THPMB048.

[13] G. Tranquille *et al.*, "The CERN-ELENA Electron Cooler Magnetic System", in *Proc. IPAC'18*, Vancouver, Canada, Apr. 2018, paper TUPAF056.

[14] G. Tranquille and J. Cenede and S. Deschamps and A. Frassier and L.V. Jørgensen, "Commissioning the ELENA Electron Cooler", in *Proc. COOL'19*, Novosibirsk, Russia, Nov. 2019, paper TUPS12.

[15] C. Gonzalez and F. Pedersen, "An ultra low noise AC beam transformer for deceleration and diagnostics of low intensity beams," in *Proc. PAC'99*, New York, NY, USA, Mar. 1999.

[16] J. Sanchez-Quesada, "ELENA Ring Longitudinal Pick-ups Commissioning Report", CERN, Geneva, Switzerland, EDMS 1740107, Jan. 2017.

[17] O. Marqversen (ed.) *et al.*, "The Orbit Measurement System for the CERN Extra Low Energy Antiproton Ring". in *Proc. IBIC'17*, Grand Rapids, Michigan, USA, Aug. 2017, paper TUPCF05.

[18] O. Marqversen and S. Jensen, "Schottky Signal from Distributed Orbit Pick-Ups," in *Proc. IBIC21*, Online, Online, Sep. 2021, paper WEPP04.

[19] P. Grandemange, "Preliminary simulation with Geant4 for the AD scraper renovation," CERN, Geneva, Switzerland, Oct. 2016.

[20] J. R. Hunt, "Beam Quality Characterisation and the Optimisation of Next Generation Antimatter Facilities," PhD Thesis, U. Liverpool, United Kingdom, 2019.

[21] M. Hori, "Photocathode Microwire Monitor for Nondestructive and Highly Sensitive Spatial Profile Measurements of Ultraviolet, X-Ray, and Charged Particle Beams", *Rev. Sci. Instrum.*, vol. 76, no. 11, p. 113303, Nov. 2005.

[22] P. Belochitskii *et al.*, "Two years of AD operation: Experience and progress", in *Proc. EPAC'02*, Paris, France, Jul. 2002, paper MOPLE081.

[23] A. Borucka and D. Gamba and A. Latina, "Comparison of available models of electron cooling and their implementations", *these proceedings*, Novosibirsk, Russia, Oct. 2021, Paper P1005.

[24] J.R. Hunt *et al.*, "Emittance Measurements in Low Energy Ion Storage Rings," *Nucl. Instr. Meth.*, vol. 896, pp. 139-151, Jul. 2018.

[25] M.E. Angoletta *et al.*, "A New Digital Low-Level RF and Longitudinal Diagnostic System for CERN's AD", in *Proc. IPAC'19*, Melbourne, Australia, May, 2019, paper TH-PRB070.

[26] M. Chanel *et al.*, "Measurements of H^- intra-beam stripping cross-section by observing a stored beam in LEAR", CERN, Geneva, Switzerland, Feb. 1987, report CERN-PS-87-012-LEA.

[27] The LEAR Team, "Epluchage des H^- dans LEAR par le gas residuel, la lumière des jauges par un faisceau laser ou une lampe spot", CERN, Geneva, Switzerland, 1987, report CERN/PS/LEA Note 87 (unpublished).

[28] B. Peart and D. S. Walton and K. T. Dolder, "Electron detachment from H^- ions by electron impact", Journal of Physics B: Atomic and Molecular Physics, Oct. 1970, pp. 1346–1356.

[29] A. Latina, "RF-Track Reference Manual", CERN, Geneva, Switzerland, 2021, https://doi.org/10.5281/zenodo.4580369.